JOURNAL OF GUIDANCE, CONTROL, AND DYNAMICS
Vol. 28, No. 2, March–April 2005

Real-Time Navigation of Formation-Flying Spacecraft Using Global-Positioning-System Measurements

Sunny Leung* and Oliver Montenbruck†
DLR, German Aerospace Research Center, 82230 Wessling, Germany

Spacecraft formation flying is commonly considered a key technology for advanced space missions. Compared with large individual spacecraft, the distribution of sensor systems to multiple platforms offers improved flexibility and redundancy, shorter times to mission, and the prospect of being more cost effective. The present study describes the design and prototype implementation of a navigation system that enables high-precision relative navigation of multiple formation-flying satellites in real time using representative space hardware. A fully decentralized system design has been adopted, in which each spacecraft is equipped with its own single-frequency global-positioning-system receiver and navigation computer. A continuous exchange of raw measurements between any two satellites in the formation is achieved through a communication architecture using multichannel radio modems operated in a time-multiplexed manner. Multiple Kalman filters running concurrently on each navigation computer provide estimates of both the local spacecraft's absolute state vector and the relative state vectors of all remote satellites in the formation. Using live global-positioning-system signals generated by a signal simulator, the proper operation of the navigation process and the communication architecture has been validated in a realistic environment. Real-time relative navigation could first be demonstrated for a formation of up to four spacecraft with an accuracy of 1.5 mm (position) and 5 μm/s (velocity) over a 4-km baseline.

Nomenclature

$\boldsymbol{a}_{\text{emp}}$	=	empirical acceleration vector, m/s^2
$\boldsymbol{B}$	=	group and phase ionospheric calibration (GRAPHIC) bias vector
b	=	GRAPHIC bias
d	=	interpolation coefficient
E	=	elevation, deg
f	=	state vector derivative, m/s and m/s^2
$\boldsymbol{g}$	=	measurement partials
I	=	ionospheric path delay, m
m	=	mapping function
N	=	carrier-phase integer ambiguity
$\boldsymbol{N}$	=	vector of carrier-phase ambiguities
$\boldsymbol{P}$	=	covariance matrix
$\boldsymbol{x}$	=	filter state vector
$\boldsymbol{y}$	=	position-velocity vector, m and m/s
$\Delta\boldsymbol{y}$	=	relative state vector, m and m/s
η	=	result of Runge–Kutta step
θ	=	fractional step size
λ	=	global-positioning-system (GPS) carrier wavelength, m
ρ	=	geometric range to GPS satellite, m
ρ^*	=	ionosphere free pseudorange, m
σ	=	measurement standard deviation, m
φ	=	GPS carrier phase, cycles

Superscripts

$\nabla\Delta$	=	double-difference operator
$+$	=	postmeasurement update value
$-$	=	premeasurement update value

Received 8 January 2004; revision received 9 May 2004; accepted for publication 15 June 2004.

*Ph.D. Candidate, German Space Operations Center; currently Engineer, GNSS Today, Ltd., Flat F, 18/F, Tower 3, Robinson Heights, 8 Robinson Road, Central, Hong Kong, People's Republic of China; sunny.leung@gnsstoday.com.

†Head, GPS Technology and Navigation Group, German Space Operations Center; oliver.montenbruck@dlr.de.

I. Introduction

IN contrast to traditional mission design and operation philosophies in which all functionalities and payloads are centralized on a single massive space platform, formation flying introduces the concepts of distribution and decentralization. The concept of distribution allows a massive satellite to be replaced by a number of smaller spacecraft operating in a formation.[1,2] Each spacecraft carries portions of the overall payloads and sensor systems to perform specific roles. Information collected by each spacecraft can be shared among others in the formation via intersatellite communication to allow for a more flexible onboard data-management scheme. With the ability to transfer information and measurements between member spacecraft, a more effective utilization of available computing resources can be achieved by techniques such as distributed computing and system load balancing. Another major benefit of a distributed architecture is the flexibility to replace or upgrade existing elements of the fleet and the ability to reconfigure the formation to meet evolving mission objectives.[3]

A fundament of formation flying with its intrinsically tight orbit control requirements is the accurate determination of the relative state (position and velocity) between individual spacecraft in real time. For satellites in low Earth orbit (LEO), the use of the global positioning system (GPS) poses an attractive alternative to other relative navigation sensors (e.g., optical metrology or radar) in terms of accuracy, robustness, flexibility, and acquisition cost. With the continuous advancement in microelectronic engineering, the size and power consumption of GPS receivers will further reduce, which makes them a perfect candidate for operation in microsatellite and nanosatellite buses. In addition, GPS provides highly accurate timing information for onboard time synchronization and enables simultaneous measurements from spacecraft within the formations.

In view of these advantages, the subject of GPS-based relative navigation for space vehicles has been addressed by many authors since the late 1990s, and carrier differential GPS (CDGPS) has been shown to offer highly accurate relative navigation solutions in theoretical studies and software simulations. Recent advances in spaceborne relative navigation were demonstrated in hardware-in-the-loop simulations using live GPS signals for orbiting spacecraft. Table 1 highlights the results obtained by various researchers and provides an overview of the current state of the art in spacecraft relative navigation for formation-flying satellites.

Table 1 Summary of CDGPS relative navigation simulations and achieved three-dimensional rms accuracies

Reference	Position, cm	Velocity	Baseline	Receiver	Processing
4	5	1 mm/s	0–10 km	GPS Architect (12 channels, UT/CSR s/w)	Real-time, desktop PC
5	6	0.5 mm/s	10 km	Dual-frontend Orion receiver	Off-line
	1	0.5 mm/s	1 km	(12 channels, MIT s/w)	
8	50	1 cm/s	12 km/s	GPS Orion receiver (12 channels, DLR s/w)	Real-time kinematic, receiver internal
7	1	n/a	1 km	Astrium Mosaic (8 channels)	Real-time, desktop PC
6	1	1 mm/s	0.6 km	ITT low-power transceiver	Off-line

Ebinuma[4] has first demonstrated precise closed-loop rendezvous of two spacecraft using relative GPS navigation and achieved an accuracy of 5 cm and 1 mm/s (three-dimensional rms) in position and velocity. A similar accuracy was later obtained in a 10-km fixed baseline scenario. The navigation filter has a dimension of 20, which includes the absolute states of the two spacecraft (target and chaser satellite) along with other modeling parameters and double-difference carrier-phase ambiguities. The relative state is computed from the difference between the two absolute state estimates. Busse[5] presented a decentralized CDGPS navigation concept designed for the Orion formation-flying microsatellite mission. The filter directly estimates the relative states from single-difference carrier-phase measurements and the known local absolute state. For a 1-km baseline separation scenario, the filter's accuracy is on the order of 1–2 cm and 0.5 mm/s (three-dimensional rms) in position and velocity. As the separation between two spacecraft increases, a systematic offset (on the order of 2–5 cm) in the relative position solution shows up, which causes a degradation in the overall three-dimensional rms accuracy. ITT has designed a GPS relative navigation algorithm for the low-power transceiver (LPT) to be flown on the TechSat-21 mission. From off-line software simulations, it is reported to provide a relative navigation accuracy on the order of 1 cm and 1 mm/s (three-dimensional rms) for position and velocity in a 600-m baseline scenario. The navigation filter processes double-difference carrier-phase measurements and employs a Bayesian estimation technique to resolve double-difference phase ambiguities.[6] Hartrampf et al.,[7] finally, have demonstrated relative navigation with an accuracy of about 1 cm (three-dimensional rms) in an ionosphere-free 1-km baseline simulation scenario. Their relative navigation algorithm processes double-difference carrier-phase measurements in a purely kinematic manner by resolving the phase ambiguities.

The preceding results clearly demonstrate the high potential of CDGPS navigation for spacecraft formation-flying applications and provide a realistic validation of fundamental algorithms both in terms of accuracy and robustness. Compared with pure software simulations and covariance studies conducted earlier, the use of spaceborne GPS receiver hardware and true GPS signals in these hardware simulations marks a major progress on the way to actual flight experiments. Considering the vision of fully autonomous, multispacecraft formation flying, various limitations can, however, be noted in the aforementioned studies. Whereas some authors have employed high-performance desktop computers for real-time simulations,[4,7] others have restricted themselves to off-line analyses of raw GPS measurements recorded in the signal simulator test bed.[5,6] In no case have the suggested navigation algorithms been executed on realistic flight computers with their inherent limitations in memory and computing performance. On the other hand, simplified DGPS algorithms for use in spaceborne GPS receivers[8] have only achieved a notably lower accuracy level. Aside from unrealistic assumptions on the available onboard computing power, most of the real-time simulations just cited have been restricted to dual-spacecraft formations or rendezvous scenarios. Therefore, fundamental questions of communication, concurrency, and scalability for multispacecraft formations have not been adequately addressed so far.

In view of these considerations, the present research has focused on the development of a real-time navigation system using representative space hardware and supporting multispacecraft operation in a fully scalable manner. A decentralized system architecture that meets these design goals is described in the following section along with the hardware components (GPS receiver, navigation computer, radio modems) employed in a prototype implementation. Subsequently, the algorithms for absolute navigation of the local spacecraft and relative navigation of the remote spacecraft are presented along with a discussion of relevant performance aspects. The report concludes with a description of hardware-in-the-loop simulations that demonstrate a superior navigation accuracy as well as a stable real-time behavior of the resulting system for formations involving up to four individual spacecraft.

II. System Concept and Prototype Implementation

A. Architectural Design

Navigation and control concepts for formation-flying satellites can traditionally be divided into centralized and decentralized concepts,[9] even though partially decentralized systems have recently been proposed as a possible compromise between the two extremes.[10] All relevant computations and decisions are taken by a master spacecraft in a centralized architecture and communicated to the remote nodes for information and/or execution. The simplicity and transparency of this approach comes at the risk of single point failures unless a hot swap can be performed in which the master role is assigned to another spacecraft in the formation. A decentralized architecture is therefore preferable, which employs identical hardware on all nodes and allows a flexible expansion (or downsizing) of the formation. Even though decentralization might be difficult to achieve in the area of formation control, it can readily be realized for the navigation task, which covers the accurate determination and prediction of absolute and relative state vectors for all satellites in the formation.

The concept of a decentralized navigation system (compare Fig. 1) implies that each spacecraft in the formation is independently equipped with its own GPS receiver, navigation computer, and radio system for intersatellite communication. Raw measurements collected by the GPS receivers are locally used to determine the absolute state vector (position and velocity) of each spacecraft. In addition, these measurements are broadcast to other satellites in the formation and can then be processed differentially to determine the relative states of two spacecraft with high accuracy. All system components used on the individual satellites must necessarily be compatible to ensure proper interoperability of all nodes. There is no general requirement, however, for using fully identical hardware, which might inhibit an extension of the formation or the replacement of individual satellites after initial deployment. Specific compatibility requirements affecting, for example, the selection of suitable GPS receivers are addressed in the subsequent sections describing the hardware components for the prototype implementation of a multispacecraft navigation system.

Although the scalability of such a system will always be limited by the employed hardware (for example, computing power or communication bandwidth), the basic architecture should be free of any restrictions concerning the number of spacecraft in the formation. In the adopted design, full scalability is achieved by a dedicated communication concept and a suitable partitioning of individual navigation functions. This allows a timewise separation of individual tasks

Table 2 Hardware components for prototype navigation system

Item	Description	Space heritage	Power, W	Reference
GPS receiver	Orion-S; 12 channels L1 C/A code and carrier	Yes	2.0	16
Preamplifier	VAS/Motorola + 28 dB	Yes	0.1	N/A
Navigation computer	Power PC 823e, 48 MHz, 66 MIPS BOSS R/T O/S	Yes	2.5	19[a]
Radio modem	ADCON MC Light, 433 MHz, 10 channels, half-duplex	No	1.5	20

[a]Data available online at http://www.first.fraunhofer.de/~sergio/public_domain/boss/bass3.html [cited 2000].

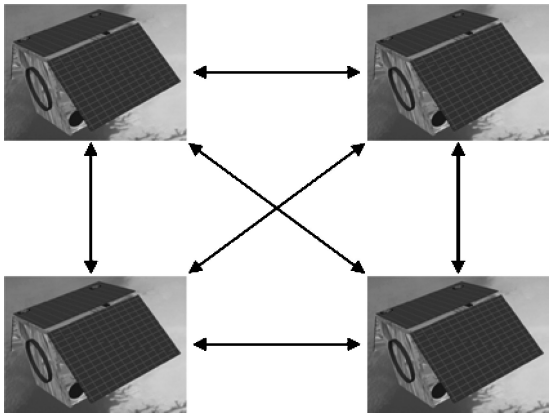

Fig. 1 Decentralized navigation system architecture for multisatellite formation flying. Each spacecraft carries identical or compatible hardware (GPS receiver, navigation computer, and radio modem), exchanges GPS measurements, and computes both of its own absolute state vectors as well as relative state vectors with respect to all other satellites in the formation.

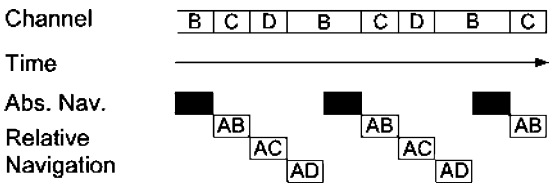

Fig. 2 Assignment of communication channels and scheduling of navigation tasks for a sample formation comprising four satellites. The local spacecraft (A) periodically receives raw GPS measurements from the remote satellites (B, C, and D), which are subsequently used to determine the relative orbits (AB, AC, and AD). Measurements from the local GPS receiver are used to determine the trajectory of spacecraft A at the beginning of each cycle. Absolute and relative state vectors are propagated and interpolated throughout a cycle to provide continuous navigation information.

instead of requiring a fully parallel data transfer and processing for all spacecraft in the formation (Fig. 2). Thus, changes in the number of active satellites affect only the overall execution time but not the number of communications ports or transmitter/receiver units required on each spacecraft.

As part of the proposed design, the communication system is assumed to support selectable channels, which can be realized using, for example, different carrier frequencies or spread spectrum technology. Each spacecraft is assigned a dedicated channel for transmission, thus allowing a fully simultaneous broadcasting of synchronized GPS measurements from all nodes in the formation. The receive channel can be switched by the navigation computer to collect measurements from a selected remote satellite for subsequent use in the relative navigation task. By sequentially receiving and processing measurements from the various channels, the navigation system can thus determine the relative states with respect to all other satellites in the formation (Fig. 2). For spacecraft in near-circular LEO, state vector updates are only required once every 30–60 s, during which the trajectory can be propagated and interpolated with adequate accuracy.[11] Making use of this fact, a

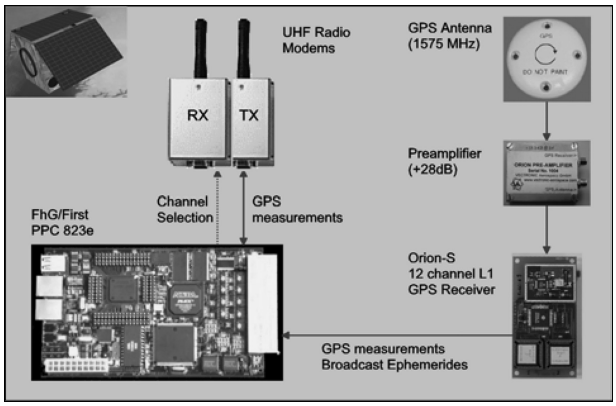

Fig. 3 Hardware components employed in the prototype implementation of the real-time navigation system. Each satellite in the formation is assumed to carry the same (or compatible) equipment. The passive GPS antenna shown here for completeness is not required in the laboratory test bed, where the preamplifier is directly connected to the signal simulator r/f output.

minimum time of 5 s per satellite is generally available for data transmission and processing. In case of maneuvers, thruster activity information can be exchanged between spacecraft and incorporated into the state propagation and filtering. A multisatellite navigation system can thus be realized even with modest computing resources and limited communication bandwidth.

For the prototype implementation, hardware components with space heritage have been selected where relevant (Table 2; Fig. 3). These are discussed in more detail in the subsequent sections.

B. GPS Receiver

Aside from its general qualification for use in low Earth orbit, a GPS receiver for use in the real-time navigation system should offer low noise code and carrier-phase tracking, ensure integer ambiguities in double-difference carrier-phase measurements, and enable proper synchronization of measurements to integer GPS seconds. Although dual-frequency measurements would be desirable to fully eliminate ionospheric effects and to facilitate carrier-phase ambiguity resolution, the limited availability and high price of adequate receivers do not render this option practical at present. All algorithms employed in the present study are therefore confined to single-frequency GPS measurements. As shown in the subsequent sections, ionospheric effects can nevertheless be eliminated to a fair degree using a specific code-carrier combination for absolute navigation and differenced-phase measurements for relative navigation.

For the prototype implementation of the formation-flying navigation system, the GPS Orion-S receiver has been selected. It has been developed based on public design information for the Mitel/Zarlink GP2000 chipset[12] and the GPS Architect software development kit.[13] The receiver employs a 12-channels hardware correlator for L1 C/A code and carrier tracking and has specifically been adapted for fast acquisition and accurate tracking in LEO applications. Critical run-time parameters and the system time are maintained by a battery-backed nonvolatile memory and real-time clock during power-down times. In combination with a built-in orbit propagator, the receiver can thus perform a warm or hot start with representative times to first fix of 30–120 s. Two serial ports are provided for

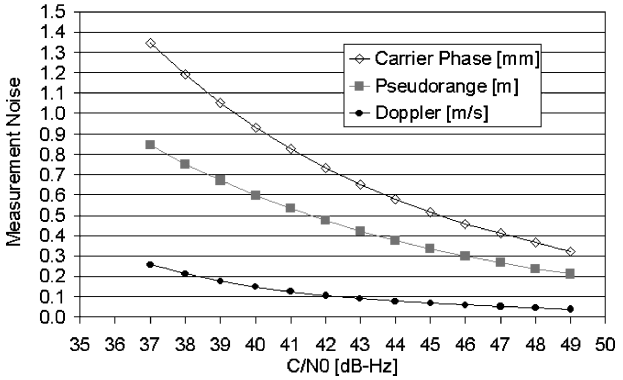

Fig. 4 Measurement noise of Orion-S receiver as derived from zero-baseline signal simulator tests for a LEO scenario.

communication with a host computer, modem, or data recorder. In addition, the original board design has been supplemented with a one-pulse-per-second (1PPS) signal line for synchronization of the spacecraft onboard time to GPS time. At a size of 95×50 mm and a power consumption of 2 W, the receiver can even be accommodated on microsatellites with limited onboard resources. The Orion GPS receiver board has been tested to tolerate a total ionizing dose of typically 15 krad, which ensures a sufficient lifetime in the radiation environment of low Earth orbits. It has so far successfully been flown on various sounding rockets and two nanosatellites.

The Orion-S receiver employs a third-order phase-locked loop and a narrowband, first-order delay lock loop with carrier aiding for precise code and carrier tracking. As demonstrated in extensive signal-simulator tests,[14,15] the measurements exhibit noise levels of 35 cm (pseudorange), 0.5 mm (carrier phase), and 0.07 m/s (Doppler) at a carrier-to-noise ratio of 45 dB-Hz (Fig. 4). Systematic measurement errors that might be encountered at high signal dynamics are avoided in the Orion-S receiver through the employed tracking loop design and a careful calibration of all measurement time tags. Aside from the raw observations, carrier smoothed pseudoranges (around 6-cm noise level) and carrier-phase-based range-rate measurements (accurate to 1–2 cm/s) are made available, which enable a smoother receiver internal navigation solution. In contrast to most other receivers based on the GP2000 chipset, the Orion-S receiver generates carrier-phase measurements with integer ambiguities in double-differenced observations. This enables the resolution of carrier-phase ambiguities in the relative navigation algorithms and overcomes a fundamental limitation of earlier studies performed by Ebinuma[4] and Busse.[5]

All measurements provided by the Orion-S receiver are synchronized to integer GPS seconds with a representative accuracy of 0.2 μs. Measurements collected by different receivers in the formation can therefore be differenced directly for the purpose of relative navigation. At an orbital velocity of roughly 7.5 km/s, the residual timing uncertainty corresponds to a maximum range error of about 1.5 mm, which slightly exceeds the carrier-phase noise but does not sacrifice the achievable navigation accuracy.

Primary output data of the Orion-S GPS receiver consist of raw pseudorange, carrier-phase, and Doppler measurements that are issued once per second in a single, ASCII encoded output message of 505 bytes length (compare Ref. 16). Using a serial radio link with a 19.2 kbaud data rate, the message can be forwarded to other satellites in the formation within about 0.25 s. This is well within the overall timing constraints of the navigation system that could even tolerate much larger delays and update intervals. A message giving the current time and the receiver internal navigation solution is generated once per second. It is used by the local navigation processor for time synchronization and during startup of the navigation filter. Finally, a broadcast ephemeris parameter message is issued on request of the user as well as autonomously in case of GPS navigation message updates for any of the tracked channels.

For completeness it is noted that the Orion receiver has recently been superceded by the Phoenix receiver,[17] which is software compatible but employs the advanced GP4020 correlator and microcontroller chip. It offers the same tracking performance and radiation tolerance at a further reduction in size (50×75 mm) and power (0.7 W) and is the candidate receiver for future flight experiments. However, all tests and simulations presented in this report have still been performed with the Orion-S receiver as just described.

C. Navigation Computer

The navigation processor employed in the present study has been designed and built by the Institute for Computer Architecture and Software Technology of the Fraunhofer Gesellschaft (FhG/First). It is based on an engineering model of the onboard computer for the BIRD microsatellite mission, which has successfully operated in space for more than two years and therefore fully representative of present day flight hardware. The eurocard-sized board features an industrial PowerPC 823e processor operated at a 48-MHz clock rate. It provides a performance of 66 million instructions per second (MIPS) but lacks a coprocessor for floating point support. For comparison, 10 MIPS were achieved by the fully radiation tolerant ERC-32 central processor employed in the PROBA (Project for Onboard Autonomy) spacecraft,[18] and a performance of 100 MIPS is expected for the LEON processor to be employed on Proba-2 in 2006 (Vuilleumier, private communication, July 2003).

A total of 8 MB of DRAM memory are available on the PowerPC processor board as well as 8 MB of shadow mirror memory and 128 kB of ROM to save critical run-time parameters.[19] The DRAM is parity protected and duplicated, which allows for error detection and correction. The navigation computer requires a 12-V supply and has a maximum power consumption of about 2.5 W. For laboratory use an external interface board has been added, which provides three serial interfaces (for connecting, e.g., the GPS receiver, radio modem, and remote PC) as well as a parallel port for software uploads. In addition, a dedicated input line is available to receive the 1PPS signal of the GPS receiver for onboard clock synchronization.

The BOSS real-time operating system employed for the navigation processor is a multithreading, preemptive operating system with fault tolerance support and has specifically been developed for safety critical applications.[‡] The operating system (as well as the application software) is implemented in C++, making extensive use of object-oriented design elements. In the PowerPC processor implementation BOSS supports a timing resolution of 1 μs, which allows a highly accurate scheduling of individual software threads.

D. Radio Modems

In the absence of suitable space-qualified hardware, commercial radio modems (transmitter and receiver pairs) are used for inter-spacecraft communication in the prototype navigation system. The MC Light radio modem[20] employed for this purpose is a frequency shift keying half-duplex FM radio transceiver (see Fig. 3). It operates in the public 433-MHz band and supports up to 10 channels with 175-kHz spacing. The serial link is configurable and is set to 40 kB/s at 19,200 baud. A simple communication protocol is used with no data collision avoidance management. The modem consumes 1.5 W at a 12-V supply voltage. It has a transmitting power of +10 dBm (10 mW) and a permitted communication range of up to 1 km. With onboard electrically erasable programmable read-only memory (EEPROM) support, configuration parameters such as channel selection, baud rate, and transmission protocol can be uploaded and stored within the modem via its RS-232 interface. The modem is controlled using the standard Hayes or AT mode command set.

Each spacecraft is assigned a dedicated transmit frequency. Thus a formation of 10 spacecraft can be handled with the 10 separate channels available on the MC Light modem. Even though each MC Light radio modem contains both a receiver and transmitter, it does not allow full duplex operation. This is incompatible with the architecture of the present system, in which each spacecraft node transmits GPS data at exactly the same times. (Note that all measurements are synchronized to integer GPS seconds.) As a work

[‡]Data available online at http://www.first.fraunhofer.de/~sergio/public_domain/boss/boss3.html [cited 2000].

around two separate modem units can be employed in each node of the navigation system, one operating in receive-only mode and one in transmit-only mode.

III. Navigation Algorithms

Following the presentation of the navigation system architecture and hardware components in the preceding section, the algorithms used to obtain filtered state vectors from the raw GPS measurements are now presented. Different processing schemes are employed for absolute and relative navigation, with the goal to minimize or eliminate measurement errors and to optimally exploit the accuracy potential of the available observations. Instead of jointly estimating the combined state vectors of all spacecraft from the cumulative set of available measurements, the state vector of the local spacecraft is first determined from code and carrier-phase observations and subsequently assumed to be known. Individual baselines to remote satellites in the formation are then determined from differential carrier-phase measurements. For both absolute navigation and relative navigation an extended Kalman filter is employed to obtain filtered state vectors at discrete time steps. In between the filter update steps, a continuous navigation solution is provided through interpolation of the propagated states.

A. Local Spacecraft Navigation

Despite the availability of single-point navigation solutions provided by the GPS receiver itself, the present navigation system is designed to independently determine the position and velocity of the local spacecraft from raw GPS measurements. Because of ionospheric path delays, the single-frequency position solutions of GPS receivers onboard LEO satellites might be in error by several tens of meters and exhibit systematic radial errors of several meters (e.g., see Refs. 21 and 22). Furthermore, the velocity solution offered by spaceborne GPS receivers is at best accurate to 1 cm/s, which does not allow a proper forecast of the trajectory in case of temporary GPS outages. In view of a strong interest in smooth, continuous, and accurate onboard position knowledge, a dedicated filter for determining the local spacecraft orbit is therefore employed in the formation-flying navigation system. Key aspects of its implementation are described in the subsequent paragraphs. For a comprehensive discussion the reader is referred to Ref. 23.

1. Trajectory Model

Within the time update step of an extended Kalman filter,[24] the spacecraft trajectory is propagated using a dynamical orbit model between consecutive measurement updates. The equation of motion adopted for this purpose accounts for the aspherical gravity field of the Earth and introduces empirical accelerations $\boldsymbol{a}_{\text{emp}} = (a_R, a_T, a_N)$ in radial, along-track, and cross-track direction to account for residual perturbations (drag, luni-solar gravity, radiation pressure, etc.) that are not explicitly modeled. As a compromise between computational efficiency and propagation accuracy, a 10×10 JGM-3 gravity field model has been implemented. Compared to a 50×50 model, a 2.5-m accuracy is achieved in predictions of up to 30 min at a 650 km altitude. Errors caused by the neglect of aerodynamic drag and luni-solar perturbations are on the order of 1 m (Ref. 23). Similar differences have, furthermore, been encountered in comparison with the trajectory model of the STR4760 GPS signal simulator that was used in all tests of the navigation system. Here, a maximum error of 1.5 m has been encountered in a 30-min prediction of a polar orbit at 450 km altitude. However, a 30×30 model would be required to achieve the same propagation accuracy at this orbital altitude in a real-world application. On the employed Power PC 823e processor the computation time for a single propagation step would then increase to roughly 2.1 s (compared to 0.3 s for the 10×10 gravity model). This is well tolerable, however, in the present design of the navigation system, which requires state updates and predictions only once every 30–60 s.

The use of large update intervals is supported through a specific numerical integration scheme, which offers a high efficiency and yields a continuous representation of the trajectory for dense (i.e., high rate) output.[11] It builds up on the classical fourth-order Runge–Kutta method (RK4) and is used for solving a first-order differential equation

$$\dot{\boldsymbol{y}} = \boldsymbol{f}[t, \boldsymbol{y}(t)] \tag{1}$$

which describes the evolution of the position-velocity vector $\boldsymbol{y} = (\boldsymbol{r}, \boldsymbol{v})$ as a function of time t, from given initial conditions $\boldsymbol{y}_0 = \boldsymbol{y}(t_0)$. Making use of the concept of Richardson extrapolation,[25] the result η_H of a single RK4 step of size H is combined with the results η_{1h} and η_{2h} of two consecutive RK4 integration steps of size $h = H/2$ to obtain fifth-order approximations

$$\hat{\boldsymbol{\eta}}_{1h} = \boldsymbol{\eta}_{1h} + \frac{\boldsymbol{\eta}_{2h} - \boldsymbol{\eta}_H}{2(2^4 - 1)}$$

$$\text{and} \qquad \hat{\boldsymbol{\eta}}_{2h} = \boldsymbol{\eta}_{2h} + \frac{\boldsymbol{\eta}_{2h} - \boldsymbol{\eta}_H}{2^4 - 1} \tag{2}$$

of the state vector at times $t_0 + 1h$ and $t_0 + 2h$. By combining the intermediate results, a quintic Hermite polynomial

$$\boldsymbol{y}(t_0 + \theta h) = d_0(\theta)\boldsymbol{y}_0 + d_1(\theta)h\boldsymbol{f}(\boldsymbol{y}_0) + d_2(\theta)\hat{\boldsymbol{\eta}}_{1h} + d_3(\theta)h\boldsymbol{f}(\boldsymbol{\eta}_{1h}) + d_4(\theta)\boldsymbol{\eta}_{2h} + d_5(\theta)h\boldsymbol{f}(\boldsymbol{\eta}_{2h}) \tag{3}$$

with coefficients[26]

$$d_0 = \tfrac{1}{4}(\theta - 1)^2(\theta - 2)^2(1 + 3\theta), \qquad d_1 = \tfrac{1}{4}\theta(\theta - 1)^2(\theta - 2)^2$$

$$d_2 = \theta^2(\theta - 2)^2, \qquad d_3 = (\theta - 1)\theta^2(\theta - 2)^2$$

$$d_4 = \tfrac{1}{4}\theta^2(\theta - 1)^2(7 - 3\theta), \qquad d_5 = \tfrac{1}{4}(\theta - 2)\theta^2(\theta - 1)^2 \tag{4}$$

can then be constructed. It provides a consistent, fifth-order approximation over the interval $[t_0, t_0 + 2h]$ with θ denoting the fractional stepsize (i.e., the time since t_0 in units of h). In case of LEO satellites with near circular orbits, the errors achieved by this integration and interpolation scheme can generally be neglected in comparison with trajectory and model errors for a (macro-)step size H of less than 60 s (compare Ref. 11).

2. Ionosphere-Free Group and Phase Ionospheric Calibration Measurements

A combination of code and carrier-phase measurements is processed in the measurement update step of the Kalman filter, which provides the opportunity to eliminate ionospheric errors in the navigation process. As suggested by Yunck,[27] an ionosphere-free linear combination, known as GRAPHIC (group and phase ionospheric calibration) measurement can be obtained from single-frequency GPS data by forming the arithmetic mean

$$\rho^* = (\rho^{C/A} + \rho^{L1})/2 = \rho + c(\delta t - \delta t_{\text{GPS}}) + b \tag{5}$$

of the coarse/acquisition (C/A) code and the L1 carrier-phase measurements

$$\rho^{C/A} = \rho + c(\delta t - \delta t_{\text{GPS}}) + I$$

$$\rho^{L1} = \lambda\varphi = \rho + c(\delta t - \delta t_{\text{GPS}}) - I + \lambda(N + \delta\varphi) \tag{6}$$

Here $c\delta t_{\text{GPS}}$ and $c\delta t$ are the GPS and receiver clock offsets, respectively, and $2b = \lambda(N + \delta\varphi)$ denotes the carrier-phase bias, which is treated as float value in the present context. The ionospheric group delay $(+I)$ affecting the code measurements is equal in size but opposite in sign to the phase change $(-I)$ and therefore cancels in the GRAPHIC data type. Another advantage consists of the reduced noise level, which is roughly one-half of the C/A code noise (i.e., around 0.2 m for the Orion-S receiver). Unfortunately, however the GRAPHIC measurement involves an unknown bias b, which inhibits its direct use in single-point navigation solutions. Only a coarse a priori value

$$b \approx (\rho^{L1} - \rho^{C/A})/2 \tag{7}$$

can be obtained from the code-carrier difference measurements by neglecting the ionospheric path delay. Its exact value must therefore be adjusted along with other parameters as part of the estimation process.

3. Kalman-Filter Implementation

With the adopted trajectory model and measurement set, a total of 22 parameters

$$\boldsymbol{x} = (\boldsymbol{y}, \boldsymbol{a}_{\text{emp}}, c\delta t, \boldsymbol{B}) \tag{8}$$

have to be processed in the Kalman filter. These include the six-dimensional spacecraft position and velocity vector $\boldsymbol{y}$, the three-dimensional empirical accelerations vector $\boldsymbol{a}_{\text{emp}}$, the GPS clock offset $c\delta t$, and a vector $\boldsymbol{B} = (b_1, \ldots, b_{12})$ comprising the GRAPHIC biases for each tracking channel of the GPS receiver.

The filter is started using the receiver internal single-point navigation solution, zero empirical accelerations, a zero clock offset, and a priori GRAPHIC biases provided by Eq. (7). Furthermore, a diagonal a priori covariance matrix $\boldsymbol{P}$ with standard deviations of 10 m (position, clock, biases), 0.1 m/s (velocity), and 5×10^{-7} m/s^2 (acceleration) is assumed.

Within the time-update phase of the extended Kalman filter, the spacecraft state vector is numerically propagated from the latest state estimate, while the remaining parameters are assumed to be constant between the epochs t_{i-1} and t_i. As just described, an interpolating polynomial is also computed as part of the propagation, which yields a continuous representation of the spacecraft trajectory for use within concurrent relative navigation tasks or other onboard applications (e.g., attitude control or geocoding of payload data). For increased computational efficiency, a Keplerian approximation of the state transition matrix $\boldsymbol{\Phi}_{yy} = \partial \boldsymbol{y}(t_i)/\partial \boldsymbol{y}(t_{i-1})$ is employed. Simplified relations are likewise employed for the remaining nontrivial block $\boldsymbol{\Phi}_{ya} = \partial \boldsymbol{y}(t_i)/\partial \boldsymbol{a}_{\text{emp}}(t_{i-1})$ of the overall transition matrix $\boldsymbol{\Phi}$. To cope with deficiencies of the employed propagation model, a fixed diagonal process noise matrix $\boldsymbol{Q}$ is considered in the time update

$$\boldsymbol{P}_i^- = \boldsymbol{\Phi}_i \boldsymbol{P}_{i-1}^+ \boldsymbol{\Phi}_i^T + \boldsymbol{Q} \tag{9}$$

of the covariance matrix. Representative process noise values used in the practical applications are $(10^{-3}\ \text{m})^2$ (position), $(10^{-6}\ \text{m/s})^2$ (velocity), $(2.5 \times 10^{-6}\ \text{m/s}^2)^2$ (acceleration), and $(3\ \text{m})^2$ (clock) for filter update intervals of 10–30 s. With these settings, the Kalman-filter "memory" is dominated by the acceleration process noise, which reflects the expected uncertainty of the dynamical model. The clock process noise, on the other hand, is based on the statistical properties of the GPS Orion-S clock offset, which is nominally aligned to zero by the receiver.

The measurement update is performed in a sequence of scalar updates rather than a single vector update using all observations at the same epoch. In this way large matrix operations of varying dimension can be avoided without sacrificing the overall operations count. Modeled observations $g(\boldsymbol{x})$ are computed using the latest position, receiver clock offset, and GRAPHIC bias for the respective tracking channel. GPS position and clock information is obtained from broadcast ephemeris parameters[28] issued by the Orion-S GPS receiver. Following Ref. 29, broadcast ephemeris errors can be expected to contribute a typical signal in space range error (SISRE) of about 1–1.5 m in real-world applications, even though somewhat larger errors have been assumed in the signal-simulator tests of the navigation system. Making use of the partial derivatives

$$\boldsymbol{g} = \frac{\partial g}{\partial \boldsymbol{x}} = \left(\frac{\partial g}{\partial \boldsymbol{r}}, 0_3^T, 0_3^T, 1, \frac{\partial g}{\partial \boldsymbol{B}} \right) \tag{10}$$

and the measurement standard deviation σ, the Kalman gain vector is obtained as

$$\boldsymbol{k}_i = \boldsymbol{P}_i^- \boldsymbol{g}_i^T \left(\boldsymbol{g}_i \boldsymbol{P}_i^- \boldsymbol{g}_i^T + \sigma^2 \right)^{-1} \tag{11}$$

which then yields the updated filter state and covariance matrix:

$$\boldsymbol{x}_i^+ = \boldsymbol{x}_i^- + \boldsymbol{k}_i \left[\rho^* - g\left(\boldsymbol{x}_i^-\right) \right], \qquad \boldsymbol{P}_i^+ = (1_{3\times 3} - \boldsymbol{k}_i \boldsymbol{g}_i) \boldsymbol{P}_i^- \tag{12}$$

Because all floating point computations inside the navigation processor are performed in double precision (eight-byte) arithmetic, no need was encountered to employ the numerically more robust Joseph algorithm or factorization methods in the filter formulation. These methods might, however, be considered in a flight implementation of the navigation filter to ensure a positive-definite covariance matrix under all conditions.

B. Relative Navigation

The Kalman filter used for relative navigation builds upon similar concepts as already described but directly estimates the relative position and velocity of a remote spacecraft from differential GPS carrier-phase measurements. In this process, the absolute state vector of the local spacecraft at the measurement is assumed to be known and can be obtained by interpolation from the absolute navigation task operated in the background. Overall errors in the local spacecraft position are generally confined to 3 m as a result of the use of ionosphere-free measurements in the navigation process. This uncertainty is comparable to broadcast ephemeris errors and contributes a maximum error of about 1.5 mm to the relative navigation solution for a 10-km baseline.[30]

1. Trajectory Model

To propagate the filtered state between measurement updates, an appropriate dynamical model for the evolution of the relative state vector between two spacecraft is required. Because the accuracy of linearized relative motions models for near-circular orbits (known as Hill's equations or Clohessy–Wiltshire equations) is incompatible with the desired navigation accuracy, a numerical trajectory model has been adopted. Given the position-velocity vector $\boldsymbol{y}$ of the local spacecraft A and the relative state $\Delta\boldsymbol{y}$ at an initial epoch t_i, the two states $\boldsymbol{y}_A = \boldsymbol{y}$ and $\boldsymbol{y}_B = \boldsymbol{y} + \Delta\boldsymbol{y}$ are independently propagated to the new epoch t_{i+1} using the fourth-order Runge–Kutta integrator with Richardson extrapolation described earlier. The propagated relative state is then obtained from the difference $\Delta\boldsymbol{y}(t_{i+1}) = \boldsymbol{y}_B(t_{i+1}) - \boldsymbol{y}_A(t_{i+1})$. Because of a high degree of common error cancellation, only the leading perturbations need to be considered in the trajectory model. The present implementation uses a JGM-3 Earth field gravity model with spherical harmonics up to degree and order 10, out of which the oblateness term ($J_2 = -C_{20}$) needs to be included as a minimum. No empirical forces need to be considered in the relative model, but a differential drag term might be added if the aerodynamic coefficients of the two spacecraft are not well enough balanced. As in the case of single spacecraft navigation, the state transition matrix

$$\Phi_{\Delta y \Delta y} = \left. \frac{\partial \Delta \boldsymbol{y}(t_i)}{\partial \Delta \boldsymbol{y}(t_{i-1})} \right| = \frac{\partial \boldsymbol{y}_B(t_i)}{\partial \boldsymbol{y}_B(t_{i-1})} \tag{13}$$

is again approximated by a Keplerian formulation.

2. Measurement Model

To fully exploit the accuracy potential of the carrier-phase measurements, a double-difference (DD) processing scheme has been adopted (Fig. 5). Denoting by

$$\nabla\Delta(*)_{\text{AB}}^{ij} = \left[(*)_B^j - (*)_A^j \right] - \left[(*)_B^i - (*)_A^i \right] \tag{14}$$

the double difference of quantities related to GPS satellites i and j as well as receivers A and B, the fundamental measurement equation can be expressed as

$$\nabla\Delta(\lambda\varphi)_{\text{AB}}^{ij} = \nabla\Delta(\rho)_{\text{AB}}^{ij} + \nabla\Delta(\lambda N)_{\text{AB}}^{ij} - \nabla\Delta(I)_{\text{AB}}^{ij} \tag{15}$$

Here, λ denotes the L1 wavelength (19.0 cm). Whereas differencing across receivers minimizes the impact of broadcast ephemeris errors and ionospheric errors, the difference across GPS satellites furthermore eliminates the user clock error $c\delta t$ and the initial fractional carrier phase $\delta\varphi$.

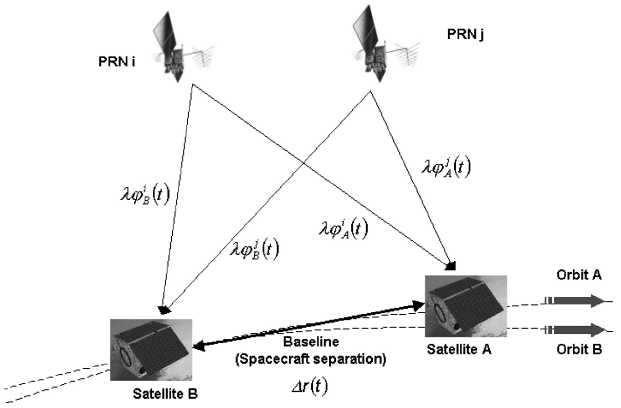

Fig. 5 Formulation of double-difference carrier-phase measurements for relative navigation of LEO satellites.

Even though the processing of DD observations implies a notable administrative overhead compared to single difference observations preferred by Busse,[5] the additional effort is well justified by the achievable gain in accuracy. Because of its integer nature, the double-difference carrier-phase ambiguity can be fixed after initial convergence of the Kalman-filter process. Fixing the ambiguities effectively converts the carrier-phase measurements into highly accurate pseudoranges and allows noise limited positioning in the absence of other errors. This advantage could not, however, be exploited in Busse's research because the design of the employed GPS receiver software did not support proper integer carrier-phase ambiguities.

Because of the use of single-frequency measurements, all carrier-phase observations are affected by ionospheric effects, and the DD carrier-phase model (15) involves a term describing the double-difference ionospheric path delay. For short separations, this delay is commonly assumed to be equal for both receivers, but this assumption is no longer valid for baselines of about 10 km, and a degradation of the relative navigation accuracy might even be encountered earlier. To overcome this difficulty, a simple analytical model[31] is employed in the present study, which describes the ionospheric path delay

$$I = I_0 \cdot m(E) \tag{16}$$

as a product of the vertical path delay I_0 and a mapping function

$$m(E) = \frac{2.037}{\sqrt{\sin^2 E + 0.076 + \sin E}} \tag{17}$$

which depends only on the local elevation E of the observed GPS satellite. Ignoring the variation of the vertical path delay over the baseline of the spacecraft, the DD carrier-phase observation can thus be modeled as a function

$$\nabla\Delta(\lambda\varphi)^{jj}_{\mathrm{AB}} = \nabla\Delta(\rho)^{jj}_{\mathrm{AB}} + \nabla\Delta(\lambda N)^{jj}_{\mathrm{AB}} - I_0\nabla\Delta(m)^{jj}_{\mathrm{AB}} \tag{18}$$

of the geometric range and parameters N and I_0 that have to be adjusted in the estimation process.

3. Filter Model

As for single satellite navigation, an extended Kalman filter is used to determine the relative state vector of two spacecraft in the formation. With the adopted trajectory model and measurement set, a maximum of 18 parameters

$$\boldsymbol{x} = (\Delta\boldsymbol{y}, I_0, \boldsymbol{N}) \tag{19}$$

have to be processed in the filter. These include the six-dimensional relative position and velocity vector $\Delta\boldsymbol{y}$, the local vertical ionospheric path delay I_0, and up to 11 double-difference carrier-phase ambiguities $\boldsymbol{N}$ for the employed 12-channel GPS receiver. The latter parameters are assumed to be constant, and only the relative state vector needs to be propagated during the state update phase. A diagonal process noise matrix is employed to compensate residual modeling deficiencies and keep the filter receptive to new measurements during extended operation. Process noise standard deviations of 0.1 mm for relative position and 0.01 μ m/s for relative velocity have been adopted for the present simulations, in which each spacecraft experiences the same drag acceleration. Increased process noise values would be required if ballistic coefficients are not well balanced and differential drag cannot be modeled properly. The propagation of I_0 and $\boldsymbol{N}$, in contrast, is considered to be error free, and no process noise needs to be introduced into the covariance for these estimation parameters.

Measurement updates are performed in a scalar manner to avoid large matrix-vector operations. If necessary, the double-difference pairs as well as the estimation parameter vector and covariance are rearranged if a single GPS satellite drops from the constellation of tracked satellites.

At startup, initial values for relative position and navigation are determined from differential pseudoranges and carrier-based differential range rates using the kinematic navigation algorithms described in Ref. 8. Coarse ambiguities are likewise obtained from the difference of code and carrier observations. A priori standard deviations are assumed as 2 m (relative position and ambiguities), 0.1 m/s (velocity), and 3 m (vertical ionospheric path delay). In the course of the filter operation, the carrier-phase ambiguities are fixed if the float ambiguity estimate lies within 2% of an integer cycle and the variation in the float ambiguity estimates within three consecutive filter updates is less than 1% of a L1 cycle. The tight constraints imposed in this process prevent an erroneous fixing of integer ambiguities, which would immediately degrade the navigation accuracy and might result in filter divergence. The relative navigation filter continuously monitors all received double-difference phase measurements. If an erroneous measurement or a cycle slip is detected for a particular double-difference phase pair with resolved integer ambiguity, the filter immediately reestimates the phase ambiguity of this GPS satellite pair. In case of a communication blackout, the filter will propagate its state using the dynamic model. The last fixed ambiguities are stored and used once communication with a remote spacecraft is reestablished. If the residual is greater than the preset limits, the filter will reestimate the ambiguity for the affected double-difference pseudo random noise (PRN) pair(s). The check is necessary to protect against any possible cycle slip during the period of communication loss.

IV. Hardware-in-the-Loop Simulations

To assess the achievable navigation accuracy and to validate the real-time operation of the navigation system, extensive tests have been conducted in a series of hardware-in-the-loop simulations (Fig. 6). GPS signals for a formation of up to four spacecraft were generated with a 48-channels Spirent STR4760 signal simulator. The spacecraft were assumed to fly in a near-circular, polar orbit at an altitude of 450 km (Table 3). The small eccentricity vector difference of spacecraft A, B, and C results in an elliptic relative motion with separations of 4 km (along track) by 2 km (radial). Spacecraft D, in contrast, exhibits a periodic out-of-plane separation of 1 km amplitude and an along-track separation of the same size. In accord with the capabilities of the signal simulator, broadcast ephemeris errors for each GPS satellite were simulated by applying

Table 3 Simulated orbital elements of the four spacecraft in the formation[a]

Element	A	B	C	D
a, km	6823.0	6823.0	6823.0	6823.0
e	0.001	0.0013	0.00118	0.001
i, deg	87.0	87.0	87.0	87.0
Ω, deg	135.0	135.0	135.0	134.991
ω, deg	0.0	0.0	12.73	0.0
M, deg	0.0	0.0	−12.73	−0.009

[a]The initial epoch is 2001/11/06 00:00:00.0 GPST (GPS week 1139; GPS seconds 172,800.0 s).

Table 4 Relative errors (three-dimensional rms) achieved after initial convergence (1500 s) of the real-time navigation system for a four-satellite formation

Pair	Position, mm	Velocity, μm/s
A–C	1.6	4.6
A–B	1.2	3.7
A–D	1.0	3.0

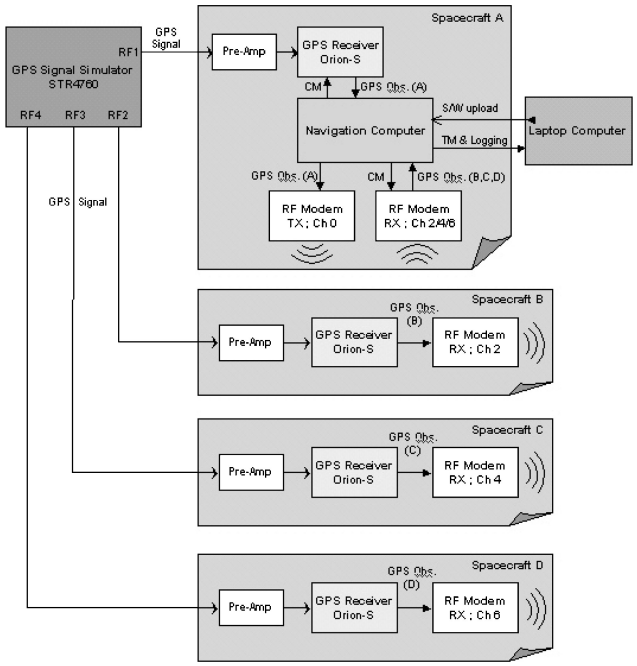

Fig. 6 Hardware-in-the-loop simulation setup for real-navigation demonstration of a four-satellite formation.

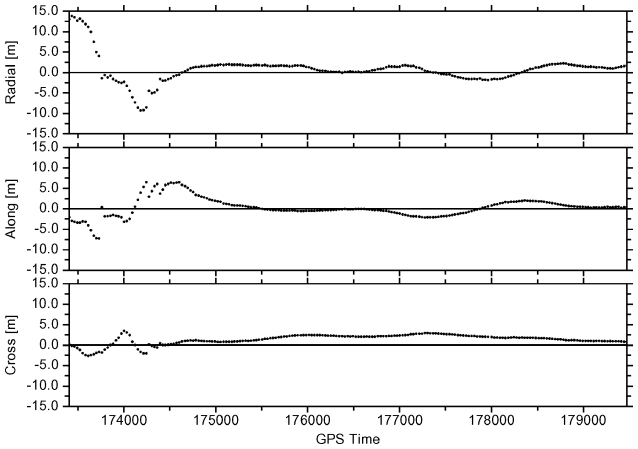

Fig. 7 Position solution errors for spacecraft A in radial, along-track, and cross-track directions. After initial convergence, the three-dimensional rms accuracy error of 2.6 m is achieved, which roughly matches the size of the simulated broadcast ephemeris error.

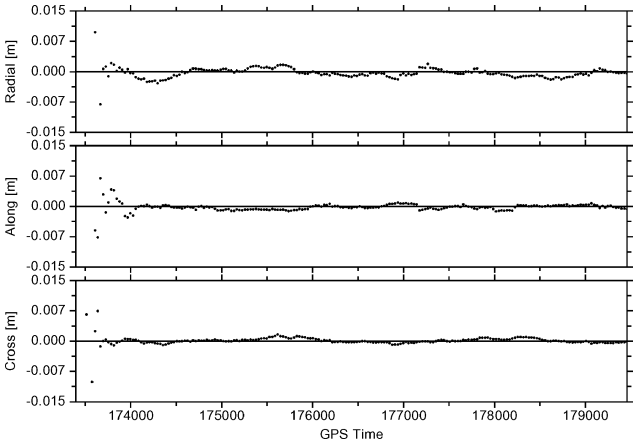

Fig. 8 Relative position solution accuracy for spacecraft pair A–C (2×4 km in-plane separation). After initial convergence, the three-dimensional rms error amounts to 1.2 mm.

independent offsets of up to 5 m (2.5 m rms) in radial, tangential, and normal direction to the simulated trajectory.[23] Furthermore, a constant electron column density of $20 \times 10^{16} e^-/m^2$ (matching a 3.2-m vertical path delay) was assumed in the simulation. On the other hand, no multipath errors have (and could) be simulated in the available environment. Although differential carrier-phase multipath can certainly be reduced by careful design of the spacecraft and antenna system, the achievable minimum is not well quantified at present, and flight data from relevant missions (e.g., GRACE, GOCE) have not yet become available. The relative navigation results obtained in our simulations should therefore be considered as those achievable in a favorable multipath environment, and some degradation might have to be expected in actual formation-flying missions.

As illustrated in Fig. 2, a total of four navigation threads were concurrently operated in the navigation processor to estimate the local spacecraft state of spacecraft A and its relative states with respect to the remote satellites B, C, and D. In all cases, filter updates were performed once per 30 s using the latest available GPS measurements. This allowed a collision-free execution of all threads on the available processor. A single absolute navigation step was completed in 3–5 s, whereas each relative state estimation step required a net processing time of 5–7 s depending on the total number of observed GPS satellites. The processor was thus operated with an idle time of roughly 10–40%.

As a consequence of the applied ionospheric and ephemeris error, the single-point navigation solution of the GPS receiver exhibits typical errors of 15 m. Making use of the GRAPHIC measurements, the navigation filter is able to remove all ionospheric errors and achieve a notably better position solution of 2.6 m (three-dimensional rms) after a convergence phase of 15–30 min (Fig. 7). This accuracy is essentially limited by broadcast ephemeris errors that cannot be fully compensated by the employed dynamical trajectory model. On the other hand, the dynamical filtering allows a clear improvement (0.34-cm/s three-dimensional rms) of the estimated velocity compared to the receiver internal solution (5-cm/s three-dimensional rms). The interpolated solution in between the 30-s Kalman-filter updates was verified to exhibit the same quality as the solution at the measurement epochs.

The relative navigation accuracy (Table 4) obtained after initial convergence of the real-time navigation process amounts to 1.5 mm (position, Fig. 8) and 5 μm/s (velocity, Fig. 9). A comparison of both values indicates a characteristic timescale of 300 s (i.e., 10 filter updates) over which measurements are averaged by the Kalman filter at the given process noise settings. The filter is therefore operated in a reduced dynamic regime, where it benefits from the low noise level of the employed carrier-phase measurements.

Following the initial convergence, the double-difference ambiguities of all (or at least most) satellites are well fixed, and the relative navigation process could even be operated in a highly kinematic mode. Here the differential position accuracy is determined by the measurement noise and amounts to roughly 5 mm for the given GPS receiver. The relative velocity error, in contrast, is proportional to the inverse filter timescale and can be adjusted via the process noise value. By (temporary) adjustment of the process noise settings, the filter can thus be made responsive to new measurements, which facilitates the filter convergence in case of orbital maneuvers.

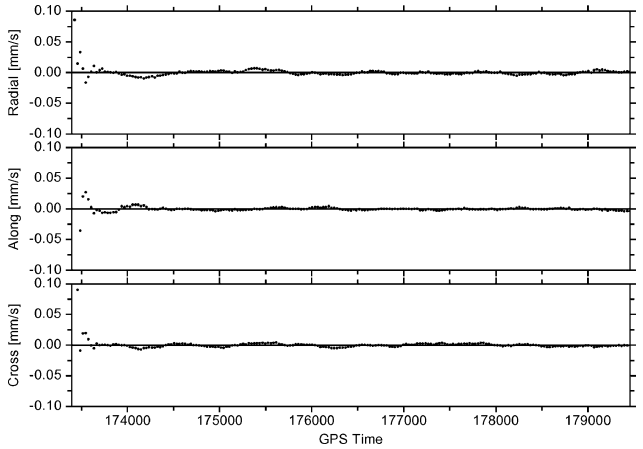

Fig. 9 Relative velocity solution accuracy for spacecraft pair A–C (2×4 km in-plane separation). After initial convergence, the three-dimensional rms error amounts to 3.7 μm/s.

At the given baseline separation of 1–4 km, systematic measurement and modeling errors are adequately compensated by the use of differential measurements and the estimation of an ionospheric delay parameter. At larger separations of 10–50 km, the relative position accuracy degrades to 1–10 cm, which is well tolerable, however, during the initial approach phase and the buildup of a formation.

V. Conclusions

The feasibility of GPS-based real-time navigation for formation-flying satellites has been demonstrated in a fully decentralized architecture using representative space hardware. Compared to previous research in this area, a superior accuracy (down to 1.5 mm and 5 μm/s for relative position and velocity) has been achieved. The improved performance can largely be attributed to the use of a more rigorous relative motion model (allowing a reduced process noise and extended filter timescale), the resolution of double-difference integer ambiguities, and the use of a GPS receiver optimized for low-noise carrier-phase tracking under space dynamics. Furthermore, ionospheric errors have been eliminated (or at least minimized) through the use of GRAPHIC measurements and the adjustment of a scaling factor for differential path delays. Both techniques effectively improve the relative navigation accuracy and help to avoid the need for dual-frequency GPS receivers in spacecraft formations with 1–10-km baselines. Overall the use of single-frequency GPS receivers appears well justified for real-time navigation of formation-flying satellites, even though dual-frequency receivers could certainly contribute to a more rapid ambiguity resolution and thus an improved convergence of the relative navigation filter.

Although all effort has been taken to provide a simulation environment as realistic as possible, the hardware-in-the-loop simulations still do not represent the true world in adequate detail. Ionospheric scintillation and large gradients of the total electron content can increase the data noise and systematic errors beyond the level of this study. Carrier-phase multipath is another limiting factor, even though the actual amount of differential multipath in a suitably designed spacecraft and antenna system has not been properly assessed so far. With these precautions the accuracies quoted in this work must therefore be considered as values achievable in practice under optimum conditions. Another limitation of the current prototype navigation system concerns the handling of maneuvers, which is not presently incorporated but will be crucial for use in orbital control and formation-keeping applications. Dedicated extensions of the communications and filter concept for the use of a priori thruster information will have to be addressed in a subsequent study.

Acknowledgments

The authors thank the ESA (ESA/ESTEC) for granting access to its Radio Navigation Laboratory and the GPS signal simulator. The given support has been essential for the hardware-in-the-loop simulations described in this report and enabled the first demonstration of GPS-based real-time navigation for a four spacecraft formation. During the development phase of the navigation system, access to a GPS signal simulator has been granted by Kaiser-Threde, Munich, which is gratefully acknowledged.

References

[1]Flower, R., and Formberg, A., "Smallsats for METOP: Design Definition, Heritage and Performance," *Acta Astronautica*, Vol. 39, Nos. 9–12, 1996, pp. 863–872.

[2]Raymond, C. A., Bristow, J. O., and Schoeberl, M. R., "Needs for an Intelligent Distributed Spacecraft Infrastructure," *Proceedings of the International Geoscience and Remote Sensing Symposium IGARSS 2002*, 2002.

[3]Das, A., and Cobb, R., "TechSat 21—Space Mission Using Collaborating Constellation of Satellites," *Proceedings of the 12th Annual AIAA/USU Conference on Small Satellites*, 1998.

[4]Ebinuma, T., "Precision Spacecraft Rendezvous Using Global Positioning System: An Integrated Hardware Approach," Ph.D. Dissertation, Univ. of Texas, Austin, TX, Aug. 2001.

[5]Busse, F. D., "Precise Formation-State Estimation in Low Earth Orbit Using Carrier Differential GPS," Ph.D. Dissertation, Dept. of Aeronautics and Astronautics, Stanford Univ., Stanford, CA, March 2003.

[6]Draganov, S., Veytsman, B., and Haas, L., "Space Applications Algorithms and Initial Simulation Results for the ITT Low-Power Transceiver," *Proceedings of the ION-GPS-2002, 15th International Technical Meeting of the Institute of Navigation*, Inst. of Navigation, Fairfax, VA, 2002, pp. 94–102.

[7]Hartrampf, M., Gottzein, E., Mittnacht, M., and Mller, C., "Relative Navigation of Satellites Using GPS Signals," *Proceedings of Deutscher Luft- und Raumfahrt Kongress*, 2002.

[8]Montenbruck, O., Ebinuma, T., Lightsey, E. G., and Leung, S., "A Real-Time Kinematic GPS Sensor for Spacecraft Relative Navigation," *Aerospace Science and Technology*, Vol. 6, No. 6, 2002, pp. 435–449.

[9]Bauer, F. H., Hartman, K., How, J. P., Bristow, J., Weidow, D., and Busse, F., "Enabling Spacecraft Formation Flying Through Spaceborne GPS and Enhanced Autonomy Technologies," *Proceedings of the ION-GPS-99, 12th International Technical Meeting of the Institute of Navigation*, Inst. of Navigation, Fairfax, VA, 1999, pp. 369–384.

[10]Carpenter, J. R., "Partially Decentralized Control Architectures for Satellite Formations," AIAA Paper 2002-4959, 2002.

[11]Montenbruck, O., and Gill, E., "State Interpolation for On-Board Navigation Systems," *Aerospace Science and Technology*, Vol. 5, No. 3, 2001, pp. 209–220.

[12]"GP2000 GPS Receiver Hardware Design," AN4855, No. 1.4, Mitel Semiconductor, Feb. 1999.

[13]"GPS Architect Software Design Manual," DM000066, No. 2, Mitel Semiconductor, April 1999.

[14]Montenbruck, O., and Holt, G., "Spaceborne GPS Receiver Performance Testing," DLR, DLR-GSOC TN 02-04, Oberpfaffenhofen, Germany, May 2002.

[15]Montenbruck, O., "Orion-S GPS Receiver Software Validation," DLR, DLR-GSOC GTN-TST-0110, Issue 1.0, Oberpfaffenhofen, Germany, June 2003.

[16]Montenbruck, O., and Markgraf, M., "User's Manual for the GPS Orion-S/-HD Receiver," DLR, DLR-GSOC GTN-MAN-0110, Issue 1.0, Oberpfaffenhofen, Germany, June 2003.

[17]Montenbruck, O., Nortier, B., and Mostert, S., "A Miniature GPS Receiver for Precise Orbit Determination of the SUNSAT2004 Micro-Satellite," *Proceedings of the ION-NTM-2004, National Technical Meeting of the Institute of Navigation*, Inst. of Navigation, Fairfax, VA, 2004, pp. 636–642.

[18]Bernaerts, D., Teston, F., and Bermyn, J., "PROBA (Project for Onboard Autonomy)," *Proceedings of the 5th International Symposium on Systems and Services for Small Satellites*, Centre National d'Etudes Spatiales, Paris, 2000.

[19]Montenegro, S., "Spacecraft Bus Computer—BIRD Spacecraft Description Vol. 3," DLR, TN-BIRD-5800-GMD/073, Berlin, May 2001.

[20]"MC Light Technical Manual," ADCON RF Technology S.A., Nice, France, 2000.

[21]Montenbruck, O., and Gill, E., "Ionospheric Correction for GPS Tracking of LEO Satellites," *Journal of Navigation*, Vol. 55, No. 2, 2002, pp. 293–304.

[22]Montenbruck, O., and Vuilleumier, P., "In-Flight Performance Analysis of the PROBA Onboard Navigation System," DLR, DLR-GSOC TN 03-02, Oberpfaffenhofen, Germany, 2003.

[23]Leung, S., "High Precision Real-Time Navigation for Spacecraft Formation Flying Using Spaceborne GPS Technology," Ph.D. Dissertation, Dept. of Aerospace Engineering, Royal Melbourne Inst. of Technology, Melbourne, Australia, Dec. 2003.

[24]Montenbruck, O., and Gill, E., *Satellite Orbits*, Springer-Verlag, Heidelberg, Germany, 2000, pp. 257–292.

[25]Hairer, E., Norsett, S. P., and Wanner, G., *Solving Ordinary Differential Equations I*, Springer-Verlag, Berlin, 1987.

[26]Sauer, R., and Szabo, I. (eds.), *Mathematische Hilfsmittel des Ingenieurs*, Vol. 3, Springer-Verlag, Berlin, 1968, pp. 248–250.

[27]Yunck, T. P., "Coping with the Atmosphere and Ionosphere in Precise Satellite and Ground Positioning," *Environmental Effects on Spacecraft Positioning and Trajectories*, edited by A. Valance Jones, Vol. 73, Geophysical Monograph Series, American Geophysical Union, Washington, DC, 1993.

[28]"Navstar GPS Space Segment/Navigation User Interfaces," Arinc Research Corp., ICD-GPS-200, Rev. C, El Segundo, CA, Sept. 1997.

[29]Warren, D. L. M., and Raquet, J. F., "Broadcast vs. Precise GPS Ephemerides: a Historical Perspective," *GPS Solutions*, Vol. 7, No. 3, 2003, pp. 151–156.

[30]Misra, P., and Enge, P., *Global Positioning System—Signals, Measurements, and Performance*, Ganga-Jamuna Press, Lincoln, MA, 2001.

[31]Lear, W. M., "GPS Navigation for Low-Earth Orbiting Vehicles," NASA 87-FM-2, Rev. 1, March 1989.